Scripta Materialia 195 (2021) 113726

Contents lists available at ScienceDirect

Scripta Materialia

journal homepage: www.elsevier.com/locate/scriptamat

Development of iron-rich microwires with a unique combination of magnetic properties

P. Corte-Leon[a,b], V. Zhukova[a,b], J.M. Blanco[b], M. Ipatov[a,b], S. Taskaev[c], J. Gonzalez[a], A. Zhukov[a,b,d,*]

[a] Dept. Advanced Polymers and Materials: Physics, Chemistry and Technology, Faculty of Chemistry, University of Basque Country, UPV/EHU, San Sebastian 20018, Spain
[b] Dpto. de Física Aplicada, EIG, UPV/EHU, San Sebastian 20018, Spain
[c] NRU South Ural State University, Chelyabinsk, Russia
[d] IKERBASQUE, Basque Foundation for Science, Bilbao 48011, Spain

ARTICLE INFO

Article history:
Received 13 November 2020
Revised 23 December 2020
Accepted 7 January 2021
Available online 20 January 2021

Keywords:
Magnetic microwires
GMI effect
Domain wall dynamics
Annealing
Internal stresses

ABSTRACT

We studied the influence of post-processing on magnetic properties of Fe-rich microwires and defined the routes to obtain Fe-rich cost-effective microwires with unique combination of magnetic properties allowing observation of fast and single domain wall, DW, propagation and Giant Magnetoimpedance, GMI, effect in the same microwire. By modifying the annealing conditions, we have identified the appropriate regimes allowing to achieve remarkable improvements in GMI ratio and single DW dynamics. The observed experimental results are discussed considering the radial distribution of the magnetic anisotropy and the correlation of the GMI effect and DW dynamics with hysteresis loops.

Magnetic materials with amorphous structure usually present excellent soft magnetic properties together with superior mechanical properties [1–3]. Such excellent combination of physical properties of amorphous materials is commonly attributed to the glassy-like structure, characterized by the absence of atomic long-range order and hence, lack of defects typical for crystalline materials, i.e., grain boundaries, dislocations, twins, etc. [1–3]. Consequently, the use of amorphous materials allows the development of robust magnetic devices and even magnetoelastic sensors and devices [4–7].

Amorphous materials can be prepared either with planar (ribbons) or cylindrical (wires) shapes [1–8]. The cylindrical geometry of amorphous materials is the most suitable for realization of either the Giant Magnetoimpedance (GMI) effect [5,7,9,10] or magnetic bistability associated with a single and large Barkhausen jump [8,11].

The principal interest in the GMI effect is related to a large sensitivity of electrical impedance to applied magnetic field (up to 10 %/A/m) observed in Co-rich amorphous microwires with vanishing magnetostriction coefficient, λ_s, [12,13]. The origin of the GMI effect is satisfactorily explained in terms of the dependence of the penetration depth, δ, of the AC current flowing through a soft magnetic conductor on the applied magnetic field [9,10]. Accordingly, a high circumferential magnetic permeability is one of the most important prerequisites for achieving a high GMI ratio [8–10].

On the other hand, spontaneous magnetic bistability is usually reported in magnetostrictive amorphous wires (i.e., for wires with either positive or negative λ_s) [8,11,14]. The magnetic bistability has been associated with the remagnetization process through a single and large Barkhausen jump [8,11,14]. In magnetically bistable wires a demagnetized state cannot be achieved, since the magnetization switching between the two remanent states runs by ultra-fast domain wall (DW) propagation. Perfectly squared hysteresis loops of magnetically bistable wires are commonly attributed to the presence of a single-domain inner core with an axial magnetization orientation.

For most magnetic sensor applications low dimensional magnetic wires are requested [5,15,16]. The thinnest amorphous wires can be prepared using Taylor-Ulitovsky method suitable for preparation of amorphous wires with metallic nucleus diameters ranging from 200 nm up to 100 μm and glass-coating thickness 0.5-20 μm [12,13,17–19].

As-prepared Co-rich microwires typically present linear hysteresis loops and hence single DW propagation in such microwires cannot be observed [13]. Less expensive as-prepared Fe-rich amorphous glass-coated microwires typically have rectangular

* Corresponding author.
E-mail address: arkadi.joukov@ehu.es (A. Zhukov).

https://doi.org/10.1016/j.scriptamat.2021.113726
1359-6462/

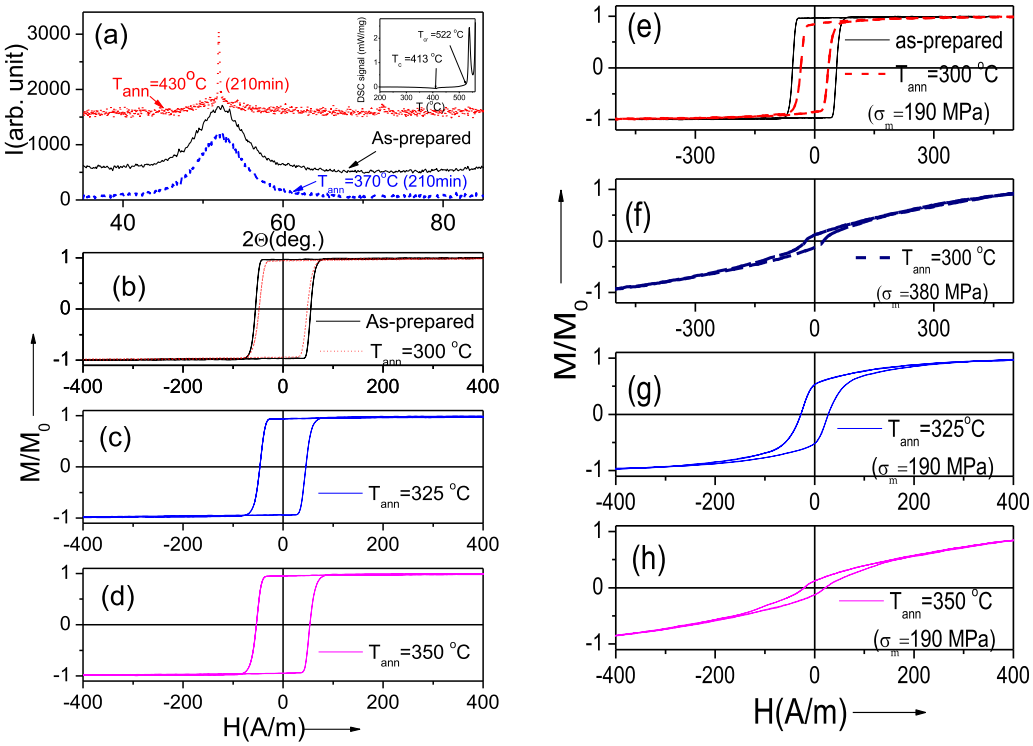

Fig. 1. XRD pattern of as-prepared and annealed $Fe_{75}B_9Si_{12}C_4$ microwires with DSC curve in the inset (a), hysteresis loops of as-prepared and annealed at T_{ann} =300 °C (b), T_{ann} =325 °C (c), T_{ann} =350 °C (d) and stress-annealed at T_{ann} =300 °C (σ_m=190 MPa) (e) T_{ann} =300 °C (σ_m=380 MPa) (f), T_{ann} =325 °C σ_m=190 MPa (g) and at T_{ann} =350 °C σ_m=190 MPa) (h) $Fe_{75}B_9Si_{12}C_4$ microwires. All heat treatments are performed for t_{ann}=60 min.

hysteresis loops with low circumferential magnetic permeability and therefore low GMI effect [20,21]. On the other hand, in Fe-rich microwires with high and positive λ_s, spontaneous magnetic bistability and, therefore, single DW propagation are observed [20,22].

The applications of GMI effect are mostly related to high sensitivity of GMI effect on magnetic field and include electronic compass for smart phones and wrist watches, biomagnetic field sensing, human magneto-cardiograms and magneto-encephalograms, non-volatile magnetic memories, magnetoelastic sensors, magnetometers as well as metamaterials [5,7,23–25]. Alternatively, magnetic bistability and related DW propagation are proposed for electronic surveillance, torque sensors, noncontact mechanocardiographs, racetrack memories, magnetic logics, etc. [8,26–29].

Recently, magnetic bistability and fast single DW propagation are reported in annealed Co-rich microwires with vanishing λ_s [20,30,31]. In spite of perfectly rectangular hysteresis loops, such annealed Co-rich microwires still present high GMI effect [20,30,31]. However, Co belongs to critical raw materials [32]. Therefore, less expensive Fe-rich microwires are preferable for industrial applications. Recently, remarkable improvement of magnetic softness and GMI effect in Fe-rich microwires achieved by induced transverse magnetic anisotropy are reported [33,34]. Such GMI effect improvement is observed in stress-annealed Fe-rich microwires with almost linear hysteresis loops in which single DW propagation cannot be observed.

The development of cost-effective glass-coated microwires, which can present a unique combination of properties: high GMI effect as well as fast single DW propagation is highly demanded by already proposed applications and can help in the creation of new applications and, therefore, it is a challenging and relevant topic of application oriented research.

In this paper, we provide our last attempts to realize the GMI effect and fast DW propagation in the same Fe-rich microwire, and present new insights on magnetization reversal mechanism in microwires exhibiting both GMI effect and fast DW propagation.

We prepared and studied $Fe_{75}B_9Si_{12}C_4$ amorphous glass-coated microwires (metallic nucleus diameter, d=15.2 μm, total diameter, D=17.2 μm) with positive λ_s, ($\lambda_s \approx 38 \times 10^{-6}$) prepared by the Taylor-Ulitovsky technique described elsewhere [12,13,30,31]. The samples were annealed in a conventional furnace. Annealing temperatures, T_{ann}, were chosen in order to preserve the amorphous structure of the samples, that is, much below the crystallization temperature [33,34].

For stress annealing, we used the same technique that was recently used for Fe-rich microwires: tensile stress was applied during heating, annealing and cooling within the furnace [33,34]. The annealing time, t_{ann}, was typically below 60 min.

The tensile stress value, σ_m, was estimated considering different Young's modulus of metal and glass, as described elsewhere [33,34]. The σ_m -value was below 200 MPa.

Amorphous character of structure has been proved by X-ray diffraction (XRD) using a BRUKER (D8 Advance) X-ray diffractometer with Cu K_α (λ=1.54 Å) radiation and by differential scanning calorimetry (DSC) performed on DSC 204 F1 Netzsch calorimeter at a heating rate of 10 K/min. The X-ray diffraction patterns of all as-prepared and annealed (at $T_{ann} \leq$370 °C for $t_{ann} \leq$210 min) microwires show a broad halo, typical of completely amorphous materials (see Fig 1a). The crystallization temperature, T_{cr}, (the first crystallization peak), estimated by DSC for as-prepared and stress-annealed $Fe_{75}B_9Si_{12}C_4$ microwire, is about 520°C (see Fig. 1a).

The hysteresis loops were measured using the fluxmetric method, previously used by us to study the soft magnetic microwire [13,20,22]. To compare the hysteresis loops of samples annealed under different conditions, we present the hysteresis loops as the dependence of the normalized magnetization, M/M_0, on the magnetic field, H, where M is the magnetic moment at a given

magnetic field, and M_0 is the magnetic moment of the sample at the maximum magnetic field amplitude, H_m.

The GMI ratio, $\Delta Z/Z$, has been defined as:

$$\Delta Z/Z = [Z(H) - Z(H_{\max})]/Z(H_{\max}), \quad (1)$$

where H_{max} is the maximum applied DC magnetic field, Z is the impedance measured using a vector network analyzer from the reflection coefficient S_{11}, as described elsewhere [35]:

$$Z = Z_0(1 + S_{11})/(1 - S_{11}), \quad (2)$$

being Z_0=50 Ohm - the characteristic impedance of the coaxial line.

The off-diagonal GMI component, $Z_{z\varphi}$, has been evaluated through transmission coefficient S_{21} [34,35].

The micro-strip sample holder used for the GMI characterization is described elsewhere [35]. The sample length for the GMI characterization is 6 mm.

The DW velocity was evaluated using a modified Sixtus-Tonks method, described elsewhere [22]. In the experimental setup, three pick-up coils are used, located coaxially along a 10 cm long microwire, which is magnetized by a long solenoid.

As mentioned above, a signature of a single DW propagation is an ideally rectangular hysteresis loop of magnetically bistable microwires associated with the remagnetization process through a single and large Barkhausen jump [8,11,14]. In such magnetically bistable microwires, the magnetization switching between the two remanent states runs by ultra-fast DW propagation. As expected, a rectangular hysteresis loop is observed in as-prepared $Fe_{75}B_9Si_{12}C_4$ microwire (see Fig. 1b). Accordingly, we are looking for post-processing (annealing or stress-annealing) that allows us to maintain perfectly rectangular hysteresis loops in the studied microwires.

Annealed (without stress for t_{ann}=60 min) $Fe_{75}B_9Si_{12}C_4$ microwires present rectangular hysteresis loops (see Fig. 1b–d). Although the character of the hysteresis loops in annealed $Fe_{75}B_9Si_{12}C_4$ microwires remains unchanged, a slight decrease in coercivity, H_c, can be observed (see Fig. 1b and c). Amorphous character of as-prepared and all annealed samples is confirmed by a broad halo observed for the samples annealed up to T_{ann}=370 °C (t_{ann} =210 min) as well as by the hysteresis loops character.

The hysteresis loops of stress-annealed (at σ_m=190 MPa or 380 MPa for t_{ann}=60 min) $Fe_{75}B_9Si_{12}C_4$ microwires change from rectangular shape to inclined with increasing T_{ann} (see Fig. 1e–h). Only the sample annealed at T_{ann} =300 °C, σ_m=190 MPa for t_{ann}=60 min presents rectangular hysteresis loop, although with lower H_c, and squareness ratio, M_r/M_o (see Fig. 1e).

As reported previously [35], the stress-annealing induced anisotropy is affected by several parameters: T_{ann}, σ_m and t_{ann}. For the shorter t_{ann}, a weaker transverse magnetic anisotropy is expected considering previous experimental results. Accordingly, stress- annealing of studied microwire at T_{ann} =325 °C, σ_m=190 MPa for shorter t_{ann} has been performed. Rectangular hysteresis loops have been observed in stress-annealed $Fe_{75}B_9Si_{12}C_4$ microwires at T_{ann} =325 °C, σ_m=190 MPa for t_{ann}=15 min and t_{ann}=30 min (see Fig. 2). Lower M_r/M_o values of stress-annealed samples have been previously attributed to increasing in the outer domain shell with transversal anisotropy at the expense of axially magnetized inner single domain [34].

Consequently, DW dynamics has been studied in the microwires presenting rectangular hysteresis loops.

Influence of annealing conditions on DW velocity, v(H), dependencies of $Fe_{75}B_9Si_{12}C_4$ microwires is shown in Fig. 3. Similarly to previous results on the effect of annealing on DW dynamics [20,36,37], a remarkable DW velocity improvement is observed upon annealing: higher DW velocities are observed after all kinds of annealing (see Fig. 3).

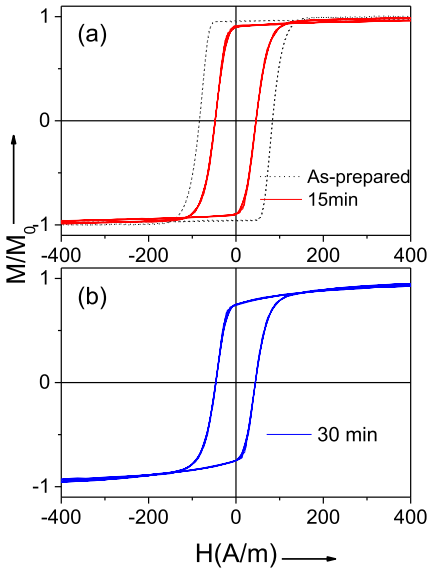

Fig. 2. Hysteresis loops of as-prepared and stress- annealed at T_{ann} = 325 °C for σ_m=190 MPa and t_{ann}=15 min (a) and t_{ann}=30 min (b) $Fe_{75}B_9Si_{12}C_4$ microwires.

Additionally, in most cases $v(H)$ dependencies can be described by a linear function.

The linear $v(H)$ dependencies observed in most microwires are described in terms of viscous DW propagation regime by the following relation [36–38]:

$$v = S(H - H_0) \quad (3)$$

being S the DW mobility, H_0 - the critical propagation field.

An increase in the DW velocity and mobility upon annealing is previously discussed considering the magnetoelastic anisotropy contribution and hence internal stresses relaxation [37,39]. Thus, magnetoelastic anisotropy contribution is evidenced by a decrease in v, with applied stress, σ_a, observed in Fe-rich microwires several times [36,39] .

On the other hand, correlation of the DW mobility, S, with the magnetoelastic anisotropy, K_{me}, and saturation magnetization, M_s, is discussed elsewhere [36–39]. Indeed, S is given by:

$$S = 2\mu_0 M_s/\beta \quad (4)$$

where μ_0 is magnetic permeability of vacuum, M_s -saturation magnetization and β- is the viscous damping coefficient.

In most of the publications, the main origin of damping in magnetic microwires is attributed to the magnetic relaxation damping, β_r, related to a delayed rotation of electrons expressed as [36,40]:

$$\beta_r \approx 2M_s\pi^{-1}(K_{me}/A)^{1/2} \quad (5)$$

where A is the exchange stiffness constant.

Accordingly, observed increase in DW mobility upon annealing (with increase of T_{ann} and t_{ann}, see Fig. 3d) must be attributed to the internal stresses relaxation associated with the annealing. Even more remarkable increase in S after stress-annealing (see Fig. 3d) must be attributed to the transverse magnetic anisotropy induced by stress-annealing. Such transverse character of stress-annealing induced magnetic anisotropy is evidenced considering core-shell model domain structure of magnetic wires [41]. Within this model, the inner axially magnetized core radius, R_c, is related to the squareness ratio, M_r/M_s as [41]:

$$R_c = R(M_r/M_s)^{1/2}, \quad (6)$$

where R is the metallic nucleus radius.

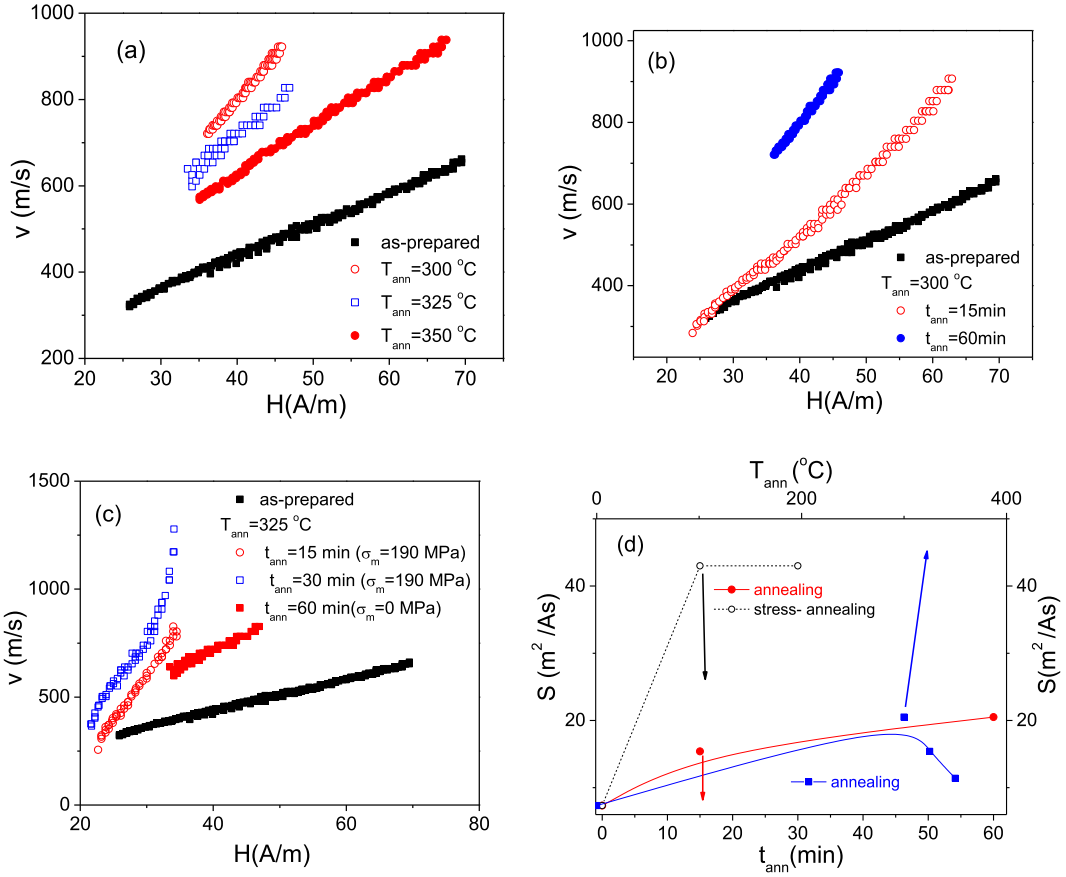

Fig. 3. v(*H*) dependences measured in as-prepared and annealed for t=60 min at different T_{ann} (a) annealed at T_{ann}=300 °C for different t_{ann} (b) annealed and stress-annealed at T_{ann}=325 °C (c) $Fe_{75}B_9Si_{12}C_4$ microwires and $S(t_{ann})$ for T_{ann}=300 °C and $S(T_{ann})$ for t=60 min dependences for annealed and stress-annealed samples.

Accordingly, a decrease in the squareness ratio observed upon stress-annealing (see Fig. 1e–h) must be attributed to an increase in the outer domain shell volume.

A more significant increase in *S* upon stress-annealing (see Fig. 3c and d) has recently been attributed to the transverse character of stress-annealing induced magnetic anisotropy [42,43]. It is assumed that the influence of transverse magnetic anisotropy on the DW dynamics of magnetic microwires is similar to the effect of an applied transverse magnetic field [43].

A weak transverse magnetic anisotropy is one of the prerequisites for achievement a high GMI effect [30,44]. Accordingly, an improvement in the GMI ratio upon stress-annealing is expected.

The comparison of $\Delta Z/Z(H)$ dependencies for as-prepared and annealed $Fe_{75}B_9Si_{12}C_4$ microwires is shown in Fig. 4a and b. A remarkable GMI ratio improvement upon stress-annealing is expected (see Fig. 4b). However, even conventional annealing (without stress) allows GMI ratio improvement (see Fig. 4a). Almost an order of magnitude increase in maximum GMI ratio, $\Delta Z/Z_{max}$, is achieved by annealing. The difference in $\Delta Z/Z(H)$ dependencies measured at 200 MHz is that a decay from H=0 is observed for annealed sample, while for the same frequency all stress-annealed samples present double-peak $\Delta Z/Z(H)$ dependencies (see Fig. 4a and b). Such double-peak $\Delta Z/Z(H)$ dependencies are the signature of transversal magnetic anisotropy (also evidenced from Fig. 1e and f).

Previously, was reported that further GMI ratio optimization can be achieved upon selection of proper frequency, *f*. Frequency dependencies of $\Delta Z/Z_{max}$ for the annealed and stress-annealed microwires are shown in Fig. 4c. As observed, the highest $\Delta Z/Z_{max}$ ≈110 % is observed for the sample stress-annealed for T_{ann} =325 °C (t_{ann} =30 min). For most of the samples, the highest $\Delta Z/Z_{max}$ is observed for *f* =300 MHz. However, several samples present high GMI ratio in a wide frequency range (see Fig. 4c).

S_{21}–values are almost zero in as-prepared sample. Both annealing and stress-annealing allow increase in off-diagonal MI effect, S_{21}, as shown in Fig. 4d. Such S_{21}–values increase must be attributed to weak transverse magnetic anisotropy in annealed samples evidenced by Fig. 4a and b.

Although the highest GMI ratio is observed in stress-annealed microwires with weak transverse magnetic anisotropy, relatively high GMI ratio is observed also in annealed Fe-rich microwires with rectangular hysteresis loops (see Fig. 4a and c). To explain such unexpectedly high GMI in annealed microwires with rectangular hysteresis loops, we must consider the importance of the damping parameter, as pointed out elsewhere [44]. Accordingly, the increase in GMI ratio observed in annealed Fe-rich microwires (see Fig. 4) can be attributed to the impact of annealing on the damping parameter, evidenced by a remarkable *S* increase after annealing (see Fig. 3).

The origin of stress-annealing induced magnetic anisotropy in Fe-rich microwires is previously discussed considering pair ordering, structural anisotropy and back-stresses mechanisms [45–47]. Bearing in mind that the studied microwire contains only one magnetic element (Fe), and recent studies of reversibility, that suggest that structural anisotropy and back stresses are the most obvious mechanisms of the observed stress-annealing induced anisotropy.

The advantage of the proposed solution is that post- processed Fe-rich microwires maintain amorphous structure presenting fast single DW propagation, improved high-frequency GMI characteristics and retaining the superior mechanical properties characteristic for amorphous materials, i.e., plasticity and flexibility.

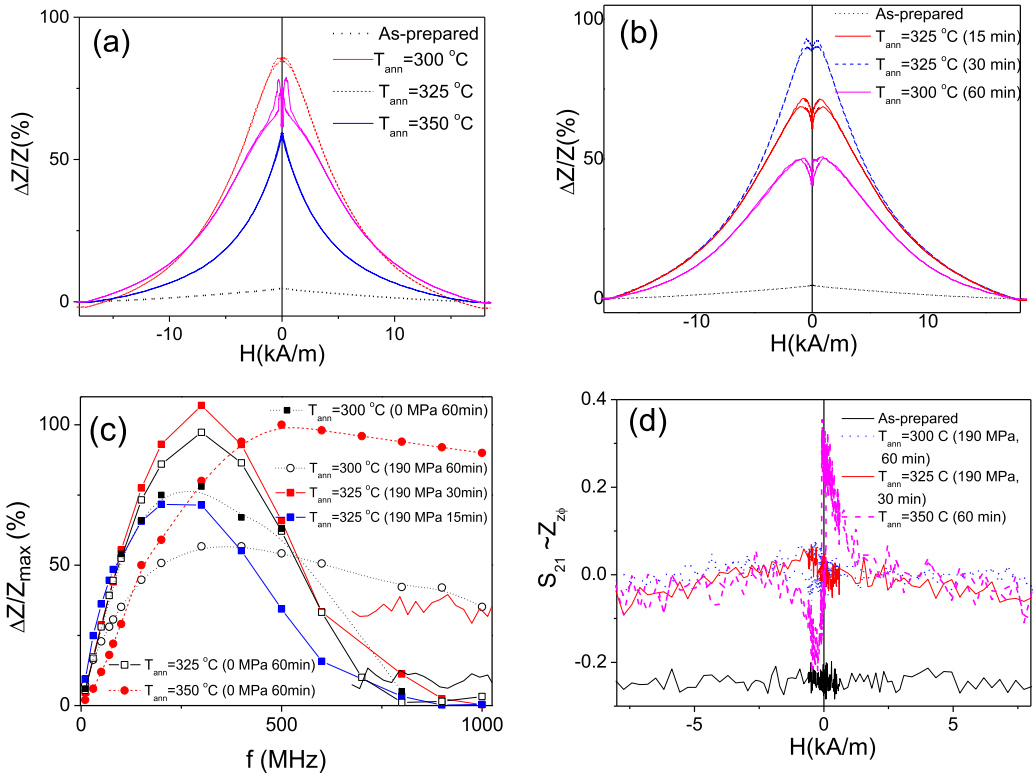

Fig. 4. $\Delta Z/Z(H)$ dependencies measured in annealed at different T_{ann} (a) and stress-annealed for σ_m=190 MPa (b) $Fe_{75}B_9Si_{12}C_4$ microwires measured at 200 MHz, $\Delta Z/Z_{max}$ (f) dependencies for annealed and stress-annealed samples (c) and $S_{21}(H)$ dependencies (d) measured in as-prepared and annealed samples at 150 MHz. $\Delta Z/Z(H)$ dependencies of as-prepared microwire are provided in Figs. 4a and b for comparison.

Concluding, by studying the influence of post-processing on magnetic properties of Fe-rich microwires we have identified the routes allowing to obtain Fe-rich cost-effective microwires with unique combination of magnetic properties, i.e., fast and single DW propagation and GMI effect in the same microwire. Under appropriate annealing conditions, we have achieved remarkable improvements in the GMI ratio and single DW dynamics. The observed experimental results are discussed considering the radial distribution of magnetic anisotropy and the correlation of GMI effect and DW dynamics with hysteresis loops.

Declaration of Competing Interest

The authors of the manuscript “Development of Fe-rich microwires with unique combination of magnetic properties.”declare no competing financial or/and non-financial interests.

Acknowledgment

This work was supported by Spanish MCIU under PGC2018-099530-B-C31 (MCIU/AEI/FEDER, UE), by the Basque Country Government under the PIBA 2018-44 and Elkartek (CEMAP and AVANSITE) projects, by the University of Basque Country under the scheme of “Ayuda a Grupos Consolidados” (Ref.: GIU18/192) and by Act 211 Government of the Russian Federation, contract # 02.A03.21.0011. The authors thank for technical and human support provided by SGIker of UPV/EHU (Medidas Magnéticas Gipuzkoa) and European funding (ERDF and ESF) .

References

[1] C.A. Schuh, T.C. Hufnagel, U. Ramamurty, Acta Mater. 55 (2007) 4067–4109.
[2] M. Hagiwara, A. Inoue, T. Masumoto, Metall. Trans. A 13 (1982) 373–382.
[3] M.E. McHenry, M.A. Willard, D.E. Laughlin, Prog. Mater. Sci. 44 (1999) 291–433.
[4] C. Morón, C. Cabrera, A. Morón, A. García, M. González, Sensors 15 (2015) 28340–28366.
[5] K. Mohri, T. Uchiyama, L.V. Panina, M. Yamamoto, K. Bushida, J. Sens. (2015) 718069, doi:10.1155/2015/718069.
[6] A. Zhukov, A.F. Cobeño, J. Gonzalez, J.M. Blanco, P. Aragoneses, L. Dominguez, Sens. Actuator A Phys. 81/1-3 (2000) 129–133.
[7] J. Nabias, A. Asfour, J.-P. Yonnet, Sensors 18 (2018) 4121.
[8] K. Mohri, F.B. Humphrey, K. Kawashima, K. Kimura, M. Muzutani, IEEE Trans. Magn. 26 (5) (1990) 1789–1791.
[9] L.V. Panina, K. Mohri, Appl. Phys. Lett. 65 (1994) 1189–1191.
[10] R. Beach, A. Berkowitz, Appl. Phys. Lett. 64 (1994) 3652–3654.
[11] D.-X. Chen, N.M. Dempsey, M. Vázquez, A. Hernando, IEEE Trans. Magn. 31 (1) (1995) 781–790.
[12] K.R. Pirota, L. Kraus, H. Chiriac, M. Knobel, J. Magn. Magn. Mater. 21 (2000) L243–L247.
[13] P. Corte-León, V. Zhukova, M. Ipatov, J.M. Blanco, J. Gonzalez, A. Zhukov, Intermetallics 105 (2019) 92–98.
[14] I. Ogasawara, S. Ueno, IEEE Trans. Magn. 31 (1995) 1219–1223.
[15] K. Mohri, T. Uchiyama, L.P. Shen, C.M. Cai, L.V. Panina, J. Magn. Magn. Mater. 249 (2001) 351–356.
[16] Y. Honkura, S. Honkura, Sensors 20 (2020) 1023.
[17] H. Chiriac, N. Lupu, G. Stoian, G. Ababei, S. Corodeanu, T.-A. Óvári, Crystals 7 (2017) 48.
[18] P. Corte-Leon, V. Zhukova, M. Ipatov, J.M. Blanco, J. González, M. Churyukanova, S. Taskaev, A. Zhukov, J. Alloys Compd. 831 (2020) 150992.
[19] L. Kraus, J. Schneider, H. Wiesner, Czech. J. Phys. B 26 (1976) 601–602.
[20] A. Zhukov, K. Chichay, A. Talaat, V. Rodionova, J.M. Blanco, M. Ipatov, V. Zhukova, J. Magn. Magn. Mater. 383 (2015) 232–236.
[21] H. Chiriac, M. Lostun, G. Ababei, T.-A. Óvári, J. Appl. Phys. 109 (7) (2011) 07B501.
[22] V. Zhukova, J.M. Blanco, P. Corte-Leon, M. Ipatov, M. Churyukanova, S. Taskaev, A. Zhukov, Acta Mater. 155 (2018) 279–285.
[23] M. Ipatov, V. Zhukova, A. Zhukov, J. Gonzalez, Sci. Rep. 6 (2016) 36180.
[24] L. Ding, S. Saez, C. Dolabdjian, L.G.C. Melo, A. Yelon, D. Ménard, IEEE Sens. 9 (2) (2009) 159–168.
[25] D. Makhnovskiy, A. Zhukov, V. Zhukova, J. Gonzalez, Adv. Sci. Technol. 54 (2008) 201–210.
[26] D.A. Allwood, G. Xiong, C.C. Faulkner, D. Atkinson, D. Petit, R.P. Cowburn, Science 309 (2005) 1688–1692.
[27] S.S.P. Parkin, M. Hayashi, L. Thomas, Science 320 (2008) 190–194.
[28] D. Makhnovskiy, N. Fry, A. Zhukov, Sens. Actuator A Phys. 166 (2011) 133–140.
[29] S. Gudoshnikov, N. Usov, A. Zhukov, V. Zhukova, P. Palvanov, B. Ljubimov, O. Serebryakova, S. Gorbunov, Phys. Status Solidi A 208 (3) (2011) 526–529.

[30] A. Zhukov, M. Ipatov, P. Corte-León, L. Gonzalez- Legarreta, M. Churyukanova, J.M. Blanco, J. Gonzalez, S. Taskaev, B. Hernando, V. Zhukova, J. Alloys Compd. 814 (2020) 152225.
[31] L. Gonzalez-Legarreta, P. Corte-León, V. Zhukova, M. Ipatov, J.M. Blanco, M. Churyukanova, S. Taskaev, A. Zhukov, J. Alloys Compd. 830 (2020) 154576.
[32] R.G. Eggert, Nat. Chem. 3 (2011) 688–691.
[33] V. Zhukova, J.M. Blanco, M. Ipatov, J. Gonzalez, M. Churyukanova, A. Zhukov, Scr. Mater. 142 (2018) 10–14.
[34] V. Zhukova, J.M. Blanco, M. Ipatov, M. Churyukanova, S. Taskaev, A. Zhukov, Sci. Rep. 8 (2018) 3202.
[35] A. Zhukov, A. Talaat, M. Ipatov, V. Zhukova, IEEE Magn. Lett. 6 (2015) 2500104.
[36] A. Zhukov, J.M. Blanco, M. Ipatov, A. Talaat, V. Zhukova, J. Alloys Compd. 707 (15) (2017) 35–40.
[37] P. Corte-León, L. Gonzalez-Legarreta, V. Zhukova, M. Ipatov, J.M. Blanco, M. Churyukanova, S. Taskaev, A. Zhukov, J. Alloys Compd. 834 (2020) 155170.
[38] R. Varga, K. Richter, A. Zhukov, V. Larin, IEEE Trans. Magn. 44 (11) (2008) 3925–3930 Part 2.
[39] V. Zhukova, J.M. Blanco, M. Ipatov, A. Zhukov, A. Phys. B 407 (2012) 1450–1454.
[40] K. Richter, R. Varga, A. Zhukov, J. Phys. Condens. Matter. 24 (2012) 296003.
[41] M. Vázquez, D.-X. Chen, IEEE Trans. Magn. 31 (2) (1995) 1229–1239.
[42] P. Corte-León, J.M. Blanco, V. Zhukova, M. Ipatov, J. Gonzalez, M. Churyukanova, S. Taskaev, A. Zhukov, Sci. Rep. 9 (2019) 12427.
[43] A. Kunz, S.C. Reiff, J. Appl. Phys. 103 (2008) 07D903.
[44] N.A. Usov, A. Antonov, A.N. Lagar'kov, J. Magn. Magn. Mater. 185 (1998) 159–173.
[45] P. Corte-Leon, V. Zhukova, J.M. Blanco, M. Ipatov, S. Taskaev, M. Churyukanova, J. Gonzalez, A. Zhukov, J. Alloys Compd. 855 (2021) 157460.
[46] F.E. Luborsky, J.L. Walter, IEEE Trans. Magn. 13 (2) (1977) 953–956, doi:10.1109/TMAG.1977.1059494.
[47] J. Haimovich, T. Jagielinski, T. Egami, J. Appl. Phys. 57 (1985) 3581–3583.